

**MINISTRY OF EDUCATION AND TRAINING
HO CHI MINH CITY UNIVERSITY OF
TECHNOLOGY AND EDUCATION**

PHAM MINH DUC

**OPTIMIZATION OF MACHINING PARAMETERS IN HARD
TURNING USING STANDARD INSERTS**

Major: Mechanical engineering

Code: 9520103

ABSTRACT OF DISSERTATION

Ho Chi Minh City, 2024

This dissertation was completed at HCMC University of Technology and Education

Supervisor 1: Associate Prof. Le Hieu Giang

Supervisor 2: Ph.D. Mai Duc Dai

Reviewer 1:

Reviewer 2:

Reviewer 3:

The dissertation was presented at the primary committee at HCMC University of Technology and Education, on

Ho Chi Minh City, 2024

ABSTRACT

Hard turning is an emerging technology for machining parts with high hardness (45 HRC and above). It offers several advantages over conventional grinding for finishing hard materials, including greater flexibility, higher productivity, lower cost, and more environmentally friendly production. However, significant challenges in hard turning involve achieving high-quality machined surfaces (low surface roughness) and minimizing cutting tool wear. Hard turning differs significantly from conventional turning, and much of the theoretical knowledge for conventional turning cannot be directly applied to hard turning. Therefore, to optimize the hard turning process, it is critical to appropriately select cutting tools (tool material and geometry) and cutting conditions (cutting speed, feed rate, depth of cut).

The primary objective of this study is to investigate the influence of the cutting tool geometric parameters (cutting edge angle, rake angle, and inclination angle) on surface roughness, tool wear, and cutting forces, and to optimize tool geometry for the hard turning process. Experimental hard turning tests were conducted on AISI 1055 steel (52 HRC) using TiN-coated ceramic cutting tools. The results indicate that the inclination angle is the major factor affecting tool wear, surface roughness, and cutting forces in hard turning. Making the rake and inclination angles more negative decreases tool wear but increases surface roughness. However, beyond a certain negative inclination angle, surface roughness begins to decrease. This finding is novel and significant in hard turning research.

Based on these results, a large negative inclination angle ($\lambda_s = -10^\circ$) is recommended to simultaneously reduce surface roughness and tool wear. Using the optimal cutting tool angles identified in this research, the hard turning process was markedly improved, with reductions in surface roughness and tool wear of 8.3% and 41.3%, respectively, compared to using standard tool angles. Mathematical models for surface roughness, tool wear, and cutting forces were also developed. Additionally, a new tool-post fixture design approach is

proposed, providing an effective method to adjust tool angles (using standard inserts) to improve the hard turning process. The new geometrical model for hard turning can be combined with other formulas to calculate local cutting forces, cutting temperatures, and tool wear for each cutting-edge element and for the overall process. It can also be applied to study the turning of other difficult-to-machine materials.

CONTENTS

CHAPTER 1: INTRODUCTION	1
1.1 Problem statement	1
1.2 Research objectives	1
1.3 Research scopes	1
1.4 Research approach and methods	2
1.5 Scientific and practical contributions	2
1.6 Thesis structure	3
CHAPTER 2: LITERATURE REVIEW	3
2.1 Introduction	3
2.2 Influence of cutting conditions in hard turning	3
2.3 Influence of tool geometry parameters in hard turning	3
2.4 Surface roughness in hard turning	3
2.5 Tool wear in hard turning	3
2.6 Mathematical modeling and optimization of the hard turning process	3
2.7 Conclusion	3
CHAPTER 3: THEORETICAL FOUNDATIONS OF THE HARD TURNING PROCESS	4
3.1 Concept of hard turning	4
3.2 Advantages and disadvantages of hard turning	4
3.3 Workpiece materials and their applications in hard turning	4
3.4 Cutting tools in hard turning	4
3.5 Cutting conditions in hard turning	5
3.6 Key economic-technical indicators in hard turning	5
3.7 Chip formation mechanism in hard turning	5
3.8 Cutting forces in hard turning	5
3.9 Cutting temperature in hard turning	5
3.10 Tool wear and wear mechanisms in hard turning	5

3.11	Tool life in hard turning	5
3.12	Conclusion	5
CHAPTER 4: MODELING OF THE HARD TURNING PROCESS		6
4.1	Introduction	6
4.2	Modeling of the hard turning process	6
4.3	Comparison of the mathematical model with the actual cutting process	7
4.4	Conclusion	8
CHAPTER 5: HARD TURNING EXPERIMENTS		8
5.1	Introduction	8
5.2	Experimental setup and parameters	8
5.2.1	Experimental equipment	8
5.2.2	Cutting tools	8
5.2.3	Experimental workpieces	9
5.2.4	Experimental parameters	9
5.2.5	Cutting conditions	10
5.3	Design and fabrication of the angle-adjustment fixture system	10
5.4	Experimental design	11
5.5	Experimental procedure	11
5.5.1	Cutting force measurement	12
5.5.2	Surface roughness (Ra) measurement	12
5.5.3	Tool Wear (VB) measurement	12
5.6	Conclusion	13
CHAPTER 6: ANALYSIS OF RESULTS AND OPTIMIZATION OF THE HARD TURNING PROCESS		13
6.1	Analysis of the geometric model of the hard turning process	13
6.2	Analysis of hard turning experimental results	15
6.2.1	Analysis and mathematical modeling of surface roughness	16
6.2.2	Analysis and mathematical modeling of tool wear	19
6.2.3	Analysis and mathematical modeling of cutting force	21

6.3	Comparison between experimental and predicted results	23
6.4	Optimization of the hard turning process	23
6.4.1	Introduction to the optimization method	23
6.4.2	The optimization problems	24
6.4.3	Comparison between standard tool angles and optimized tool angles	26
6.5	Conclusion	27
CHAPTER 7: CONCLUSIONS AND RECOMMENDATIONS		27
7.1	Conclusions	27
7.2	Future research directions	29

CHAPTER 1: INTRODUCTION

1.1 Problem statement

Hard turning, a novel machining method, is employed for finishing operations on materials with hardness ranging from 45 to 70 HRC, offering an alternative to traditional grinding processes. Due to significant differences between hard turning and conventional turning, much of the knowledge and theory developed for conventional turning cannot be directly applied to hard turning [1]. Therefore, research on hard turning continues to be actively pursued and developed.

1.2 Research objectives

The primary objective of this research is to analyze the influence of tool geometry parameters on surface roughness, tool wear, and cutting forces in hard turning using standard inserts and subsequently optimize these tool angles. The specific goals include:

- Developing a mathematical model of tool geometry for the hard turning process.
- Proposing a method for adjusting tool angles of standard inserts to optimize the hard turning process.
- Experimentally investigating the concurrent effects of tool geometry parameters (cutting edge angle, rake angle, and inclination angle) on surface roughness, tool wear, and cutting forces in hard turning.
- Establishing mathematical models relating surface roughness (Ra), tool wear (VB), and cutting force (F) to these tool geometry parameters.
- Optimizing tool geometry parameters to enhance the performance of hard turning applications using standard inserts.

1.3 Research scopes

This study focuses on:

- Investigating the influence of tool geometry parameters (cutting edge angle, rake angle, and inclination angle) on tool wear, surface roughness,

and cutting force in hard turning, under conditions in which only the tool nose radius portion engages in the cutting process ($d_w \leq r(1 - \cos K_r)$).

- Optimizing the tool angles for hard turning using standard ceramic inserts.

1.4 Research approach and methods

Theoretical and experimental research methodology.

1.5 Scientific and practical contributions

Scientific contributions:

- This is the first study to simultaneously analyze the impact of three critical tool geometry parameters (cutting edge angle, rake angle, and especially inclination angle) on tool wear, surface roughness and cutting force, which are among the most significant performance characteristics in hard turning. The predominant trends and interaction effects of these parameters on cutting force, surface roughness, and tool wear have been identified.
- Mathematical models have been established to describe the relationships of surface roughness (Ra), tool wear (VB), and cutting force (F) to the tool geometry parameters.
- Optimal tool angles for hard turning have been determined, thereby improving the hard turning process by reducing both workpiece surface roughness and tool wear compared to the standard angles provided by tool manufacturers.
- A novel geometric mathematical model for hard turning has been developed to accurately represent the inherent nature of the hard turning process. This proposed model can be combined with other equations and mathematical models to calculate cutting force, cutting temperature, and tool wear for each cutting edge element as well as for the entire process. It may also be utilized for studies on other difficult-to-machine materials.

Practical contributions:

- The proposed fixture design method provides an effective approach for adjusting tool angle parameters of standard inserts to optimize the turning process of hard or difficult-to-machine materials.
- The recommended optimal tool geometry parameters identified in this research can be practically implemented to extend tool life and achieve superior surface finish quality in hard turning operations.
- The findings of this study can be directly implemented in industrial production to improve the efficiency and effectiveness of hard turning processes.

1.6 Thesis structure

CHAPTER 2: LITERATURE REVIEW

2.1 Introduction

2.2 Influence of cutting conditions in hard turning

2.3 Influence of tool geometry parameters in hard turning

2.4 Surface roughness in hard turning

2.5 Tool wear in hard turning

2.6 Mathematical modeling and optimization of the hard turning process

2.7 Conclusion

Existing studies on hard turning have comprehensively analyzed the effects of cutting parameters, clearly identifying feed rate as the most significant factor influencing surface roughness, cutting speed as the critical determinant of tool life, and depth of cut as the primary factor affecting cutting force. However, research investigating the simultaneous effects of tool geometry parameters, particularly the inclination angle, on surface roughness and tool wear remains limited. Ceramic inserts have been recognized as the optimal cutting tool material from both economic and technical perspectives. Surface roughness and tool wear are regarded as the most critical indicators of machining quality, with mechanical

abrasion identified as the dominant wear mechanism. The experimental design method (Central Composite Design—CCD), mathematical modeling approach (Response Surface Methodology—RSM), and multi-objective optimization technique (Desirability Function Approach—DFA) are effective and commonly used research methodologies. However, further comprehensive investigation into tool geometry optimization is still necessary.

CHAPTER 3: THEORETICAL FOUNDATIONS OF THE HARD TURNING PROCESS

3.1 Concept of hard turning

Hard turning is defined as a turning process applied to workpieces with hardness values of 45 HRC or higher [67], [68]. Tool geometry and cutting conditions are critical factors influencing the effectiveness of the hard turning process.

3.2 Advantages and disadvantages of hard turning

Compared to conventional grinding, hard turning offers notable advantages, such as higher productivity, greater flexibility, lower costs, and improved environmental friendliness.

3.3 Workpiece materials and their applications in hard turning

Hard turning is typically applied to metallic materials with hardness values of 45 HRC or higher, including hardened steels, tool steels, bearing steels, high-speed steels, alloy steels, mold steels, and alloyed cast irons.

3.4 Cutting tools in hard turning

The primary cutting tool materials used in hard turning are cemented carbides, ceramics, and cubic boron nitride (CBN). Key characteristics of these tool materials include high hardness, good impact resistance, physical and chemical stability at elevated temperatures, and effective thermal conductivity. The geometry of cutting tools encompasses cutting edge angle, rake angle, inclination angle, nose radius, and cutting-edge shape.

3.5 Cutting conditions in hard turning

The key cutting parameters in hard turning include cutting speed, feed rate, and depth of cut.

3.6 Key economic-technical indicators in hard turning

3.7 Chip formation mechanism in hard turning

A distinctive characteristic of hard turning is the formation of serrated chips.

3.8 Cutting forces in hard turning

Cutting forces significantly increase when machining materials with hardness values exceeding 45 HRC, commonly considered the lower threshold for hard turning processes.

3.9 Cutting temperature in hard turning

Most of the cutting energy is converted into thermal energy, resulting in elevated cutting temperatures ranging from 800 to 1200 °C, depending on workpiece and tool materials, cutting parameters, and tool geometry. Such high temperatures directly affect machining efficiency and tool life.

3.10 Tool wear and wear mechanisms in hard turning

The primary tool wear mechanisms in machining processes include abrasive wear, diffusive wear, and adhesive wear.

3.11 Tool life in hard turning

Tool life is governed primarily by surface roughness (Ra) and flank wear (VB). According to ISO 3685, tool life concludes when surface roughness exceeds 1.6 μm or flank wear reaches 0.3 mm, with surface roughness typically serving as the primary criterion in hard turning processes.

3.12 Conclusion

This study has comprehensively presented the theoretical foundations of hard turning, a machining process that effectively substitutes traditional grinding for hardened materials (45 HRC or higher). Hard turning offers advantages such as high productivity, flexibility, and environmental friendliness; however, it also faces challenges such as significant cutting forces

and elevated temperatures, which accelerate tool wear. Commonly used tool materials include cemented carbide, ceramic, and cubic boron nitride (CBN), all of which require high thermal stability and wear resistance. Tool geometry parameters and cutting conditions decisively influence machining quality and process efficiency.

CHAPTER 4:

MODELING OF THE HARD TURNING PROCESS

4.1 Introduction

4.2 Modeling of the hard turning process

A summary of the mathematical model for tool geometry in hard turning is presented as follows:

- Local cutting-edge angle:

$$K_r^j = K_r - \theta^j \quad \text{at } \theta^j \leq K_r$$

$$K_r^j = \theta^j - K_r \quad \text{at } \theta^j > K_r$$

- Local rake angle:

$$\gamma_o^j = \tan^{-1} \left(\sin \left(\frac{\pi}{2} - \theta^j \right) \tan \gamma_o + \cos \left(\frac{\pi}{2} - \theta^j \right) \tan \lambda_s \right)$$

- Local normal rake angle:

$$\tan \gamma_n^j = \tan \gamma_o^j \cos \lambda^j$$

- Local inclination angle:

$$\lambda^j = \tan^{-1} \left(-\cos \left(\frac{\pi}{2} - \theta^j \right) \tan \gamma_o + \sin \left(\frac{\pi}{2} - \theta^j \right) \tan \lambda_s \right) \quad \text{at } \theta^j \leq K_r$$

$$\lambda^j = -\tan^{-1} \left(-\cos \left(\frac{\pi}{2} - \theta^j \right) \tan \gamma_o + \sin \left(\frac{\pi}{2} - \theta^j \right) \tan \lambda_s \right) \quad \text{at } \theta^j > K_r$$

- Portion of the tool nose radius engaged in the cutting process:

$$\theta_A = K_r - \cos^{-1} \left(\frac{r - d_w}{r} \right)$$

$$\theta_C = K_r$$

$$\theta_D = K_r + \sin^{-1} \left(\frac{f}{2r} \right)$$

$$\theta_B = K_r - \tan^{-1} \left(\frac{r \sin(K_r - \theta_A) - f}{r - d_w} \right)$$

- The angle θ_c^j in the tool rake plane:

$$\theta_c^j = \tan^{-1} \left(\frac{\tan \theta^j \cos \lambda_s}{\cos \gamma_n - \tan \theta^j \sin \gamma_n \sin \lambda_s} \right) \quad \text{at } \theta^j < \frac{\pi}{2}$$

$$\theta_c^j = \tan^{-1} \left(\frac{\tan \theta^j \cos \lambda_s}{\cos \gamma_n - \tan \theta^j \sin \gamma_n \sin \lambda_s} \right) + \pi \quad \text{at } \theta^j > \frac{\pi}{2}$$

- Uncut chip thickness:

$$\text{Zone 1: } \theta_A \leq \theta^j < \theta_B$$

$$t_1(\theta^j) = r - \frac{r - d_w}{\cos(K_r - \theta^j)}$$

$$\text{Zone 2: } \theta_B \leq \theta^j \leq \theta_D$$

$$t_2(\theta^j) = r - \sqrt{r^2 + f^2 - 2rf \cos \left(\theta^j + \frac{\pi}{2} - K_r - \sin^{-1} \left(\frac{f}{r} \sin \left(\theta^j + \frac{\pi}{2} - K_r \right) \right) \right)}$$

- Local Cutting Layer Area:

$$dA^j = t(\theta^j) r d\theta \quad \text{với giá số } d\theta$$

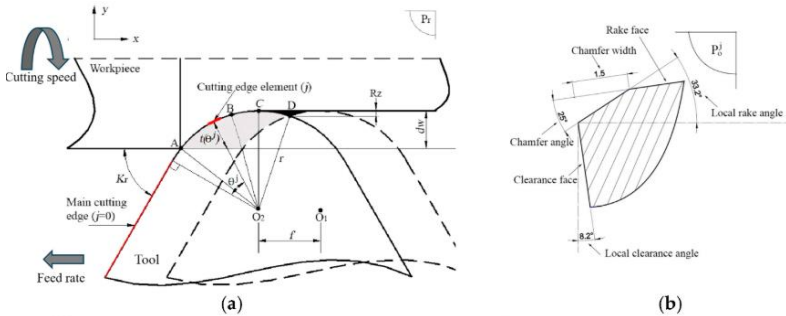


Figure 4.3 Mathematical model of nose radius approximation for cutting-edge elements in hard turning

4.3 Comparison of the mathematical model with the actual cutting process

The developed mathematical model was validated through a comparison with the actual cutting process, demonstrating good agreement and reliability.

4.4 Conclusion

The proposed mathematical model accurately describes the fundamental characteristics of the hard turning process by approximating the nose radius into primary and secondary cutting edges without limitation on the number of elements. Unlike existing models, this approach effectively captures the complex nature of hard turning. Input technological parameters, including tool geometry and cutting conditions, were integrated into the model, enabling precise predictions of cutting-edge positions, local tool geometry parameters, and local uncut chip thicknesses, key factors for analyzing, evaluating, and optimizing hard turning processes.

CHAPTER 5: HARD TURNING EXPERIMENTS

5.1 Introduction

5.2 Experimental setup and parameters

5.2.1 Experimental equipment

The hard turning experiments were conducted on a BOEHRINGER DUS-400ti CNC lathe, featuring an 11kW spindle power and a rotational speed range of 2 to 3000 rpm. The machine provides a positional accuracy of 0.001 mm.

5.2.2 Cutting tools

The cutting tools used in these experiments were standard ISO TNGA160408S01525 6050 inserts, composed of a mixed ceramic (70% Al₂O₃ and 30% TiC) coated with PVD-TiN (Figure 5.2), mounted on a standard ISO PTGNR 1616H 16 tool holder (Figure 5.3). When installed on this standard holder, the insert achieves the following tool angles: rake angle $\gamma_0 = -6^\circ$; inclination angle $\lambda_s = -6^\circ$ and cutting edge angle $K_r = 91^\circ$.

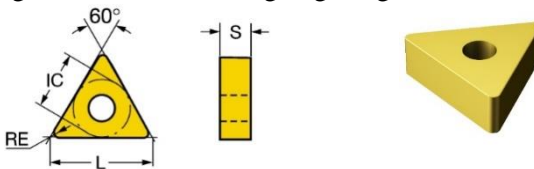


Figure 5.2 Specifications of the TNGA160404S01525 6050 insert [102]

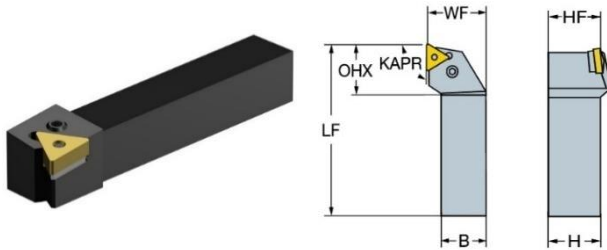


Figure 5.3 Specifications of the PTGNR 1616H 16 tool holder [102]

5.2.3 Experimental workpieces

The experimental samples were round bars of AISI 1055 steel, hardened to 52 ± 1 HRC (Figure 5.4). The dimensional characteristics of these samples are illustrated in Figure 5.5.



Figure 5.4 Experimental workpieces

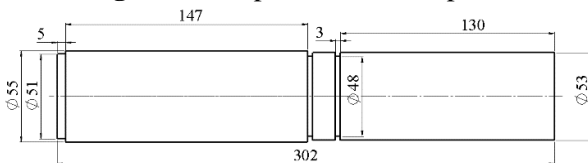


Figure 5.5 Workpiece dimensions

5.2.4 Experimental parameters

- Cutting edge angle: $60^\circ \leq K_r \leq 90^\circ$
- Rake angle: $-2^\circ \leq \gamma_o \leq -10^\circ$
- Inclination angle: $-2^\circ \leq \lambda_s \leq -10^\circ$

5.2.5 Cutting conditions

Table 5.5 The fixed cutting conditions used in the experiment

Cutting speed v (m/min)	Feed rate f (mm/rev)	Depth of cut d_w (mm)
120	0.08	0.2

5.3 Design and fabrication of the angle-adjustment fixture system

An angle-adjustment fixture system was designed using SolidWorks (Figure 5.6) and fabricated on a DMG MORI DMU65 monoBLOCK 5-axis milling machine. Dimensional verification was performed using a Hexagon GLOBAL Classic coordinate measuring machine (CMM), as illustrated in Figure 5.7. Subsequently, the fixture components underwent vacuum hardening treatment to enhance durability.

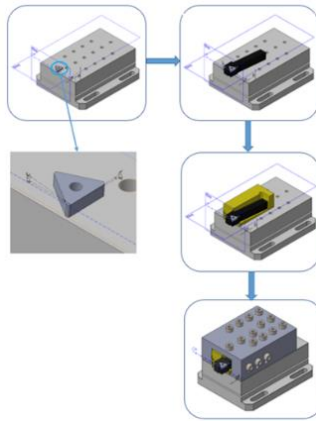


Figure 5.6 Fixture system design process for the case: $\gamma_o = -6^\circ$, $\lambda_s = -2^\circ$

The fixture system design process was conducted based on the standard "T-hand-S" system, comprising the following steps:

Step 1: Position the main cutting edge parallel to the reference plane P_r and establish the cutting edge angle K_r relative to the machine axis (x-axis), adjusting both the rake angle and the inclination angle accordingly.

Subsequently, fix the tool nose point—the point on the cutting tool closest to the machine axis—at a standardized position, specifically at a vertical distance

of 25 mm from the top surface of the fixture system (reference plane) and at a longitudinal distance of 20 mm from the end face.

Step 2: Assemble the tool holder with the cutting insert.

Step 3: Install the shim with the tool holder.

Step 4: Complete the final fixture assembly.



Figure 5.7 Fabrication process of the angle-adjustment fixture components

5.4 Experimental design

The RSM and CCD (Table 5.6) was employed in this study.

Table 5.6. Experimental design based on CCD

Tool geometry parameter	Unit	Levels				
		$-\alpha$	-1	0	$+1$	$+\alpha$
Kr	(°)	60	66	75	84	90
γ	(°)	-2	-3.6	-6	-8.4	-10
λ	(°)	-2	-3.6	-6	-8.4	-10

5.5 Experimental procedure

The experimental setup is presented in Figure 5.9.



Figure 5.9 Experimental setup diagram

5.5.1 Cutting force measurement

Cutting forces were measured in three directions (axial (F_x), radial (F_y), and tangential (F_z)) using a Kistler Type 9257B dynamometer. The cutting force measurement setup is depicted in Figure 5.12.



Figure 5.12 Cutting force measurement in hard turning

5.5.2 Surface roughness (R_a) measurement

Surface roughness was measured using a MITUTOYO SJ-210 roughness tester (Figure 5.15). This device provides a measurement accuracy of $0.001 \mu\text{m}$.

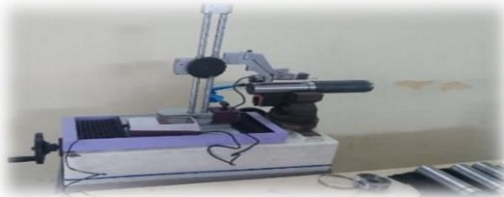


Figure 5.15 Surface roughness measurement on the test specimen

5.5.3 Tool Wear (VB) measurement

Tool wear was measured using an Oxion Inverso microscope (Figure 5.16), integrated with Amscope software, enabling high-accuracy observation and measurement of tool wear (resolution of $0.01 \mu\text{m}$).



Figure 5.16 Tool wear measurement

5.6 Conclusion

CHAPTER 6:

ANALYSIS OF RESULTS AND OPTIMIZATION OF THE HARD TURNING PROCESS

6.1 Analysis of the geometric model of the hard turning process

Hard turning is a finishing operation characterized by high cutting speeds, low feed rates, and a depth of cut not exceeding 0.2 mm [111–114]. Based on the analysis of the mathematical model for tool geometry in hard turning, the cutting action is limited to the tool nose radius (Figure 6.1).

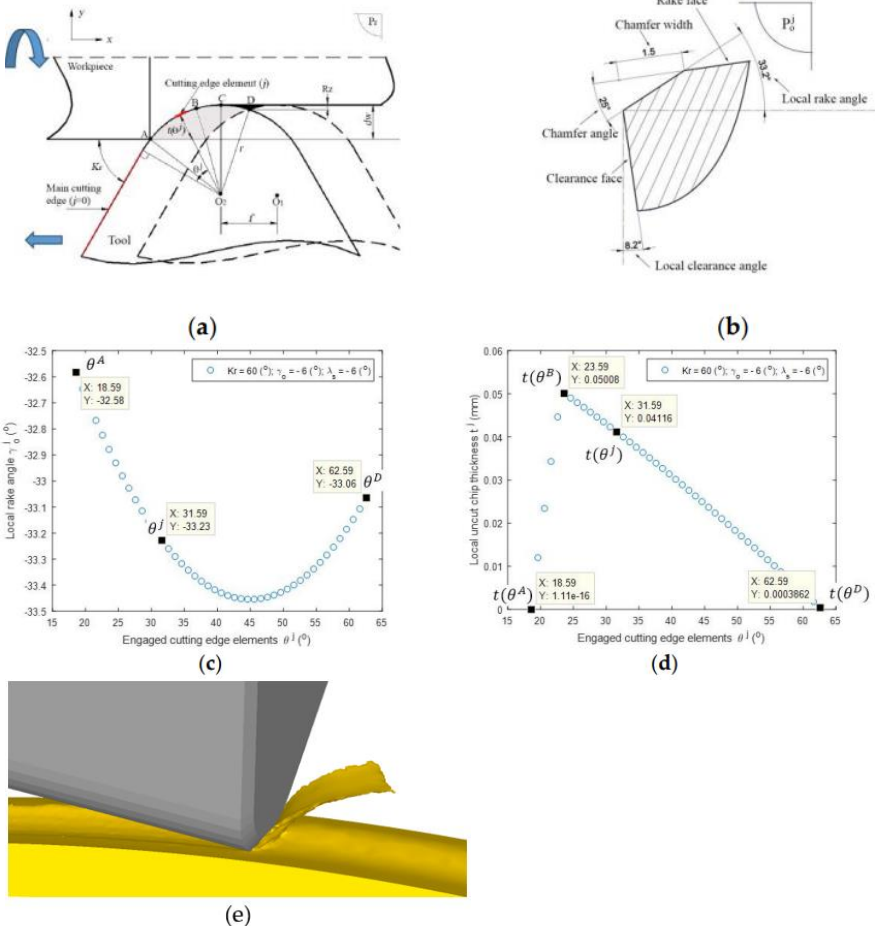


Figure 6.1 Analysis of the hard turning process for experiment no. 10

- (a) Hard turning configuration; (b) Cutting edge element geometry j at $\theta^j=31.59^\circ$; (c) Local rake angles; (d) Local uncut chips; (e) Cutting process based on FEM simulation

At each cutting point, the tool geometry parameters and uncut chip thickness vary. Due to the very small depth of cut, the chip only contacts the chamfered face of the cutting edge, resulting in a significantly large local rake angle. As shown in Figure 6.1(d), the cutting process proceeds from $\theta^A = 18.59^\circ$ to $\theta^D = 62.59^\circ$. At the cutting edge element $\theta^D = 23.59^\circ$, the maximum uncut chip thickness is $t(\theta^B) = 0.05$ mm.

Table 6.2 ANOVA for the average rake angle (γ_{ave})

Source	DF	Seq SS	Contribution	Adj SS	Adj MS	F-Value	P-Value
Model	9	73.7959	99.98%	73.7959	8.1995	6783.94	0.000
Linear	3	72.5213	98.26%	72.5213	24.1738	20000.32	0.000
Kr	1	0.7243	0.98%	0.7243	0.7243	599.22	0.000
γ	1	23.1987	31.43%	23.1987	23.1987	19193.58	0.000
λ	1	48.5984	65.84%	48.5984	48.5984	40208.15	0.000
Square	3	0.1496	0.20%	0.1496	0.0499	41.26	0.000
Kr*Kr	1	0.1483	0.20%	0.1426	0.1426	118.01	0.000
$\gamma^*\gamma$	1	0.0006	0.00%	0.0007	0.0007	0.60	0.458
$\lambda^*\lambda$	1	0.0007	0.00%	0.0007	0.0007	0.60	0.458
2-Way Interaction	3	1.1250	1.52%	1.1250	0.3750	310.26	0.000
Kr* γ	1	0.7200	0.98%	0.7200	0.7200	595.70	0.000
Kr* λ	1	0.4050	0.55%	0.4050	0.4050	335.08	0.000
$\gamma^*\lambda$	1	0.0000	0.00%	0.0000	0.0000	0.00	1.000
Error	10	0.0121	0.02%	0.0121	0.0012		
Lack-of-Fit	5	0.0121	0.02%	0.0121	0.0024	*	*
Pure Error	5	0.0000	0.00%	0.0000	0.0000		
Total	19	73.8080	100.00%				

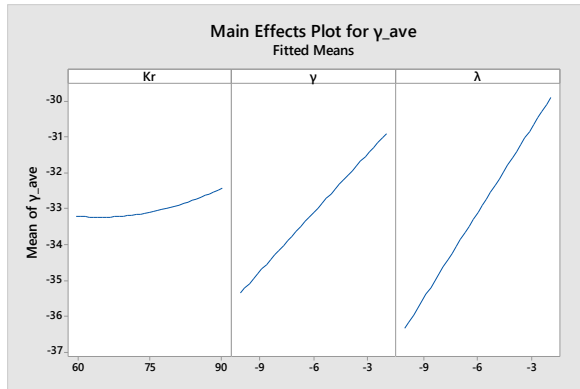


Figure 6.2 Main effects of input factors on the average rake angle γ_{ave}

Table 6.2 shows the ANOVA results for the average rake angle. The findings indicate that the inclination angle has the greatest influence at 65.84%, followed by the rake angle, contributing 31.43%. The cutting edge angle has only a 0.98% effect on the average local rake angle. Consequently, to optimize the hard turning process, attention should focus primarily on adjusting the inclination angle and rake angle. The cutting edge angle can be disregarded because of its negligible effect. The main effect plots for the average rake angle are presented in Figure 6.2. Increasing the negative rake and inclination angles leads to a higher local rake angle of the cutting edge elements at the nose radius participating in the cutting action.

6.2 Analysis of hard turning experimental results

The experimental outcomes are presented in Table 6.3.

Table 6.3 experimental results based on the CCD experimental design

STT	κ_r (°)	γ_o (°)	λ_s (°)	F_x (N)	F_y (N)	F_z (N)	F (N)	Ra (μm)	VB (μm)
1	84	-3.6	-3.6	47.19	134.92	90.91	169.40	0.279	44.04
2	66	-3.6	-3.6	45.52	123.68	84.44	156.52	0.730	44.82
3	84	-8.4	-3.6	47.11	122.86	86.24	157.33	0.594	35.98
4	66	-8.4	-3.6	46.02	118.23	83.28	151.76	0.866	32.24
5	84	-3.6	-8.4	45.47	122.67	85.13	156.08	0.720	31.24
6	66	-3.6	-8.4	41.67	116.44	82.68	148.76	0.899	32.00
7	84	-8.4	-8.4	43.28	117.09	83.17	150.00	1.004	30.12
8	66	-8.4	-8.4	42.70	119.69	82.76	151.65	0.890	23.54
9	90	-6.0	-6.0	46.00	119.87	84.80	153.87	0.836	37.80
10	60	-6.0	-6.0	41.64	117.28	81.14	148.56	0.995	29.27
11	75	-2.0	-6.0	39.19	128.71	86.89	160.16	0.766	42.11
12	75	-10.0	-6.0	43.07	116.37	81.79	148.62	1.020	27.70
13	75	-6.0	-2.0	50.69	139.00	92.28	174.38	0.252	50.26
14	75	-6.0	-10.0	48.26	125.33	87.47	160.27	0.767	22.20
15	75	-6.0	-6.0	50.67	118.66	87.13	155.69	0.870	31.85
16	75	-6.0	-6.0	51.75	119.92	85.59	156.16	0.853	32.01
17	75	-6.0	-6.0	50.72	120.02	87.02	156.68	0.852	32.33
18	75	-6.0	-6.0	52.91	118.47	86.88	156.15	0.906	32.93
19	75	-6.0	-6.0	52.07	118.44	85.11	154.86	0.919	31.63
20	75	-6.0	-6.0	50.83	118.56	85.45	154.73	0.876	31.92

6.2.1 Analysis and mathematical modeling of surface roughness

The analysis in Table 6.4 shows that the inclination angle (λ_s) has the greatest impact on surface roughness, accounting for 32.54%, followed by the rake angle (γ_o) and the cutting edge angle (K_r) at 11.88% and 9.97%, respectively. The second-order coefficient $\lambda_s \times \lambda_s$ and the interactions $K_r \times \lambda_s$ and $K_r \times \gamma_o$ also significantly affect surface roughness, contributing 31.95%, 6.6%, and 3.39%, respectively.

Table 6.4 ANOVA for surface roughness (Ra)

Source	DF	Seq SS	Contribution	Adj SS	Adj MS	F-Value	P-Value
Model	9	0.803015	97.89%	0.803015	0.089224	51.49	0.000
Linear	3	0.446212	54.39%	0.446212	0.148737	85.83	0.000
K_r	1	0.081797	9.97%	0.081797	0.081797	47.20	0.000
γ_o	1	0.097448	11.88%	0.097448	0.097448	56.23	0.000
λ_s	1	0.266966	32.54%	0.266966	0.266966	154.06	0.000
Square	3	0.270963	33.03%	0.270963	0.090321	52.12	0.000
$K_r * K_r$	1	0.006131	0.75%	0.001256	0.001256	0.72	0.415
$\gamma_o * \gamma_o$	1	0.002692	0.33%	0.000026	0.000026	0.02	0.905
$\lambda_s * \lambda_s$	1	0.262140	31.95%	0.262140	0.262140	151.27	0.000
2-Way	3	0.085840	10.46%	0.085840	0.028613	16.51	0.000
Interaction							
$K_r * \gamma_o$	1	0.027848	3.39%	0.027848	0.027848	16.07	0.002
$K_r * \lambda_s$	1	0.054120	6.60%	0.054120	0.054120	31.23	0.000
$\gamma_o * \lambda_s$	1	0.003872	0.47%	0.003872	0.003872	2.23	0.166
Error	10	0.017329	2.11%	0.017329	0.001733		
Lack-of-Fit	5	0.013506	1.65%	0.013506	0.002701	3.53	0.096
Pure Error	5	0.003823	0.47%	0.003823	0.000765		
Total	19	0.820344	100.00%				

The main and interaction effects of the tool angle parameters on surface roughness are presented in Figure 6.3. As the rake angle and inclination angle become more negative, surface roughness increases. However, when the inclination angle exceeds a specific threshold ($\lambda_s = -8.1^\circ$), surface roughness begins to decrease, as shown in Figure 6.3(a). This is a noteworthy new finding in the study of hard turning.

This phenomenon can be explained as follows: increasing the negative inclination and rake angles results in a more negative local rake angle and, correspondingly, a larger local relief angle. The inclination angle dominates this effect, as previously analyzed in the mathematical model of hard-turning tool geometry. A more negative local rake angle increases the chip–tool rake face contact length and the chip compression ratio (CCR), inducing vibration and raising surface roughness. This observation aligns with findings reported by Singh et al. [22]. However, Singh et al. only varied the local rake angle by using inserts with different chamfer angles.

Conversely, a larger local relief angle reduces the contact area between the tool flank and the freshly machined surface, thereby decreasing friction caused by the material's elastic spring-back [115], mitigating vibrations, and thus improving surface roughness, consistent with research by Senthikumar [116]. Beyond a certain threshold, the positive effect of the larger local relief angle outweighs the negative effect of the more negative local rake angle, ultimately reducing surface roughness. In other words, optimal tool angles enhance the efficiency of the cutting process.

Surface roughness also decreases as the cutting edge angle K_r increases, consistent with the results of Sharma [25] and Zerti [61]. The reason is that altering K_r from 60° to 90° changes the cutting position on the tool nose radius while reducing the local rake angle of the cutting edge elements, as previously analyzed, thereby lowering surface roughness. Nevertheless, Neseli et al. [24] reported that the cutting edge angle and surface roughness increase in parallel. This discrepancy may result from differences in whether the cutting action predominantly occurs at the tool nose radius or along the main cutting edge.

The mathematical model expressing the relationship between surface roughness and tool geometry parameters is given by equation (6.1):

$$Ra = 3.581 - 0.0654 \kappa_r + 0.1495 \gamma_o - 0.0806 \lambda_s + 0.000117 \kappa_r^2 + 0.00024 \gamma_o^2 - 0.02373 \lambda_s^2 - 0.002731 \kappa_r \gamma_o - 0.003808 \kappa_r \lambda_s - 0.00382 \gamma_o \lambda_s \quad (6.1)$$

The correlation coefficient (R^2) of regression equation (6.1) is 97.89%, indicating that the model exhibits high predictive accuracy. The effects of cutting tool angles on surface roughness, as well as the response surfaces illustrating the relationship between surface roughness, inclination angle, and tool cutting-edge angle, with a constant rake angle are presented in Figures 6.3 and 6.4.

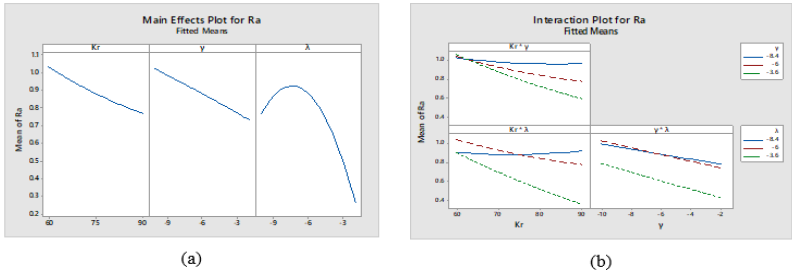


Figure 6.3. Effect plots for surface roughness

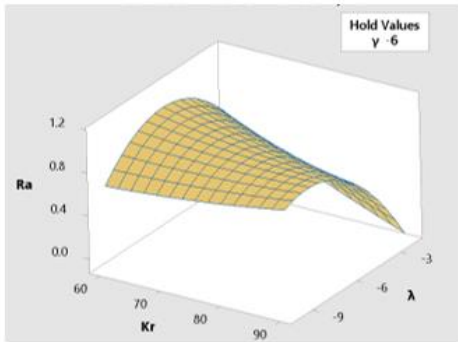


Figure 6.4. Response surface of surface roughness vs. cutting edge and inclination angles in hard turning

6.2.2 Analysis and mathematical modeling of tool wear

From Table 6.5, it is evident that the inclination angle is also the principal factor affecting tool wear, accounting for 60.06%, followed by the rake angle at 23.37%, and the side cutting edge angle at 4.2%. Other factors have negligible effects.

Table 6.5 ANOVA for tool wear (*VB*)

Source	DF	Seq SS	Contribution	Adj SS	Adj MS	F-Value	P-Value
Model	9	878.361	94.60%	878.361	97.596	19.45	0.000
Linear	3	813.702	87.63%	813.702	271.234	54.06	0.000
K_r	1	39.013	4.20%	39.013	39.013	7.78	0.019
γ_o	1	217.004	23.37%	217.004	217.004	43.25	0.000
λ_s	1	557.684	60.06%	557.684	557.684	111.15	0.000
Square	3	30.764	3.31%	30.764	10.255	2.04	0.172
$K_r * K_r$	1	0.314	0.03%	1.478	1.478	0.29	0.599
$\gamma_o * \gamma_o$	1	6.932	0.75%	9.382	9.382	1.87	0.201
$\lambda_s * \lambda_s$	1	23.518	2.53%	23.518	23.518	4.69	0.056
2-Way	3	33.895	3.65%	33.895	11.298	2.25	0.145
Interaction							
$K_r * \gamma_o$	1	17.582	1.89%	17.582	17.582	3.50	0.091
$K_r * \lambda_s$	1	1.022	0.11%	1.022	1.022	0.20	0.661
$\gamma_o * \lambda_s$	1	15.290	1.65%	15.290	15.290	3.05	0.111
Error	10	50.173	5.40%	50.173	5.017		
Lack-of-Fit	5	49.108	5.29%	49.108	9.822	46.12	0.000
Pure Error	5	1.065	0.11%	1.065	0.213		
Total	19	928.534	100.00%				

As illustrated in Figure 6.5, tool wear decreases as the rake angle and inclination angle become more negative and as the side cutting edge angle decreases from 90° to 60°. This outcome can be explained by the corresponding increase in the local clearance angle, achieved by reducing the cutting edge angle and increasing the negative rake and inclination angles, as analyzed in the mathematical model of tool geometry described previously. An increased local clearance angle reduces the contact area and friction between the newly

machined surface and the tool flank due to the elastic spring-back of the workpiece material. Consequently, flank wear is mitigated.

The mathematical model describing the relationship between flank wear VB and the input factors is presented in Equation (6.2). The model's correlation coefficient $R^2=94.6\%$, indicates a high level of predictive accuracy.

$$VB = 126.8 - 0.92 \kappa_r + 9.96 \gamma_o + 8.05 \lambda_s + 0.00401 \kappa_r^2 + 0.142 \gamma_o^2 + 0.225 \lambda_s^2 - 0.0686 \kappa_r \gamma_o - 0.0166 \kappa_r \lambda_s + 0.240 \gamma_o \lambda_s \quad (6.2)$$

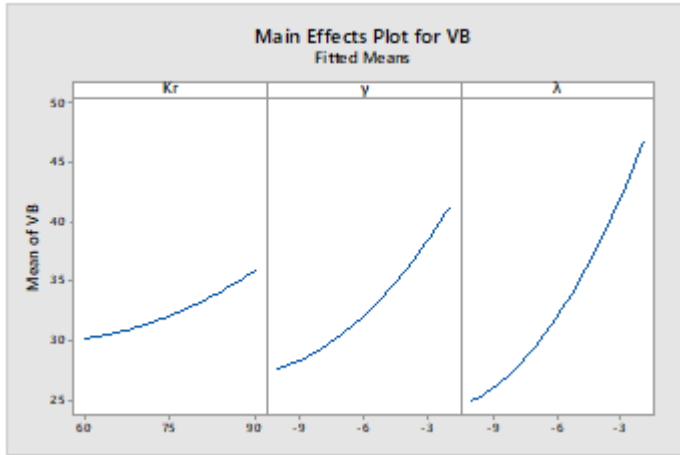


Figure 6.5 Main effect plots for flank wear (VB)

6.2.3 Analysis and mathematical modeling of cutting force

From Table 6.1, it is evident that the radial force (F_y) is the largest component, followed by the tangential force (F_z), while the axial force (F_x) is the smallest. This finding aligns with previous studies conducted by Khamel [8], Azizi [117], and Bouacha [118]. Geometrically, this phenomenon can be explained by the relatively large tool nose radius ($r = 0.8$ mm) combined with a small depth of cut ($d_w = 0.2$ mm), which causes cutting to occur primarily at the tool nose radius, resulting in a larger radial force (F_y) compared to other force components. Moreover, variations in cutting force observed when adjusting tool geometry parameters remain moderate in this study ($F = 148-174$ N).

Table 6.6 demonstrates that the inclination angle exerts the greatest effect on the cutting force, accounting for 25.02%, followed by the rake angle

at 14.26%, and the cutting edge angle at 10.04%. Although interaction effects among tool angles exist, their influence on the cutting force is relatively minor (ranging from 2.56% to 4.15%).

Table 6.6 ANOVA for Cutting Force (F)

Source	DF	Seq SS	Contribution	Adj SS	Adj MS	F-Value	P-Value
Model	9	762.048	95.52%	762.048	84.672	23.70	0.000
Linear	3	393.520	49.33%	393.520	131.173	36.72	0.000
K_r	1	80.132	10.04%	80.132	80.132	22.43	0.001
γ_o	1	113.801	14.26%	113.801	113.801	31.86	0.000
λ_s	1	199.587	25.02%	199.587	199.587	55.87	0.000
Square	3	291.768	36.57%	291.768	97.256	27.22	0.000
$K_r * K_r$	1	81.986	10.28%	66.961	66.961	18.74	0.001
$\gamma_o * \gamma_o$	1	26.617	3.34%	15.262	15.262	4.27	0.066
$\lambda_s * \lambda_s$	1	183.165	22.96%	183.165	183.165	51.27	0.000
2-Way Interaction	3	76.761	9.62%	76.761	25.587	7.16	0.007
$K_r * \gamma_o$	1	33.120	4.15%	33.120	33.120	9.27	0.012
$K_r * \lambda_s$	1	20.408	2.56%	20.408	20.408	5.71	0.038
$\gamma_o * \lambda_s$	1	23.232	2.91%	23.232	23.232	6.50	0.029
Error	10	35.723	4.48%	35.723	3.572		
Lack-of-Fit	5	32.703	4.10%	32.703	6.541	10.83	0.010
Pure Error	5	3.021	0.38%	3.021	0.604		
Total	19	797.772	100.00%				

As illustrated in Figure 6.7, the cutting force (F) decreases when the inclination angle and the rake angle increase in the negative direction. However, once the inclination angle surpasses a certain threshold ($\lambda_s = -7.2^\circ$), the cutting force begins to increase. According to the mathematical model of tool geometry in hard turning, this behavior can be explained as follows:

increasing the negative inclination angle and the negative rake angle leads to a more negative local rake angle and a corresponding local clearance angle. Consequently, the normal force and frictional force acting on the rake face increase, whereas those acting on the flank face decrease, reaching equilibrium at $\lambda_s = -7.2^\circ$, where the cutting force is minimized.

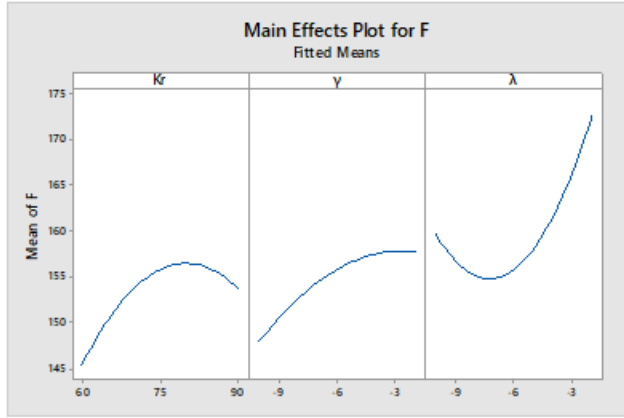


Figure 6.7 Main effect plots for cutting force (F)

The second-order regression equation describing the relationship between the input factors and the cutting force is as follows:

$$F_x = -171.2 + 5.067 \kappa_r - 9.53 \gamma_o - 0.23 \lambda_s - 0.03249 \kappa_r^2 - 0.6250 \gamma_o^2 - 0.1034 \lambda_s^2 + 0.0220 \kappa_r \gamma_o - 0.0093 \kappa_r \lambda_s - 0.0344 \gamma_o \lambda_s \quad (R^2=95.43\%) \quad (6.3)$$

$$F_y = 35.1 + 2.62 \kappa_r - 2.16 \gamma_o + 6.64 \lambda_s - 0.00976 \kappa_r^2 + 0.111 \gamma_o^2 + 0.712 \lambda_s^2 + 0.0894 \kappa_r \gamma_o + 0.0708 \kappa_r \lambda_s + 0.329 \gamma_o \lambda_s \quad (R^2=93.19\%) \quad (6.4)$$

$$F_z = -39.0 + 3.071 \kappa_r - 3.18 \gamma_o + 0.61 \lambda_s - 0.01666 \kappa_r^2 - 0.1486 \gamma_o^2 + 0.1974 \lambda_s^2 + 0.0321 \kappa_r \gamma_o + 0.0381 \kappa_r \lambda_s + 0.0857 \gamma_o \lambda_s \quad (R^2=94.35\%) \quad (6.5)$$

$$F = -48.3 + 5.325 \kappa_r - 6.26 \gamma_o + 5.36 \lambda_s - 0.02697 \kappa_r^2 - 0.1811 \gamma_o^2 + 0.6273 \lambda_s^2 + 0.0942 \kappa_r \gamma_o + 0.0739 \kappa_r \lambda_s + 0.296 \gamma_o \lambda_s \quad (R^2=92.52\%) \quad (6.6)$$

6.3 Comparison between experimental and predicted results

6.4 Optimization of the hard turning process

6.4.1 Introduction to the optimization method

This study employs the Desirability Function Approach (DFA) for optimization. Since surface roughness and tool wear are the most critical performance characteristics in hard turning, while the cutting force is relatively low and less significant for energy optimization, the focus here is on optimizing tool angle parameters to achieve the desired surface roughness and tool wear.

If the objective is to minimize the output response Y_i , then the objective function d_i can be expressed as follows:

$$d_i = \begin{cases} 1 & \text{khi } Y_i < \text{Low}_i \\ \left(\frac{\text{High}_i - Y_i}{\text{High}_i - \text{Low}_i} \right)^r & \text{khi } \text{Low}_i \leq Y_i \leq \text{High}_i \\ 0 & \text{khi } Y_i > \text{High}_i \end{cases} \quad (6.9)$$

If the objective is to achieve a specific target value (T_i), the objective function d_i is defined as follows:

$$d_i = \begin{cases} 0 & \text{khi } Y_i < \text{Low}_i \\ \left(\frac{Y_i - \text{Low}_i}{T_i - \text{Low}_i} \right)^r & \text{khi } \text{Low}_i \leq Y_i < T_i \\ \left(\frac{\text{High}_i - Y_i}{\text{High}_i - T_i} \right)^r & \text{khi } T_i \leq Y_i \leq \text{High}_i \\ 0 & \text{khi } Y_i > \text{High}_i \end{cases} \quad (6.10)$$

6.4.2 The optimization problems

a. Problem 1

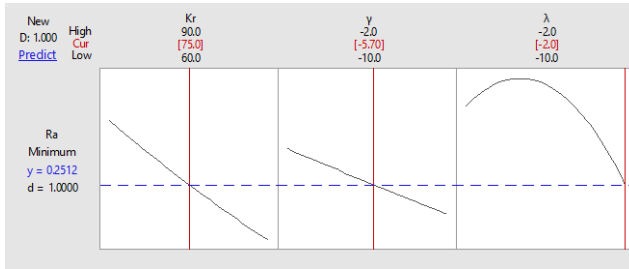
One of the primary objectives of this research is to optimize tool angles to achieve the lowest possible surface roughness, a critical factor in hard turning. Therefore, Equation (6.9) is applied, where Y_i represents the output response for surface roughness (Ra), as described by Equation (6.1).

Subject to the constraints:

$$0.25 \mu\text{m} < Ra < 1.6 \mu\text{m}; 60^\circ \leq \kappa_r \leq 90^\circ; -2^\circ \leq \gamma_o \leq -10^\circ; -2^\circ \leq \lambda_s \leq -10^\circ$$

By applying Equation (6.9), the optimal solution is presented in Figure 6.10, yielding optimal tool angles of $\kappa_r = 75^\circ$, $\gamma_o = -5.7^\circ$ and $\lambda_s = -2^\circ$. The minimum achievable surface roughness is $Ra = 0.252 \mu\text{m}$.

Figure 6.10 Optimization of surface roughness (Ra)



b. Problem 2

Another essential objective is to optimize tool angles to simultaneously achieve desired levels of surface roughness and tool wear. Accordingly, Equation (6.10) is used, where Y_i represents the output responses for surface roughness (Ra) and tool wear (VB), as described by Equations (6.1) and (6.2), respectively.

Subject to the constraints:

$$0.25 \mu\text{m} < Ra < 1.6 \mu\text{m}, 0 \mu\text{m} < VB < 0.3 \mu\text{m},$$

$$60^\circ \leq \kappa_r \leq 90^\circ, -2^\circ \leq \gamma_o \leq -10^\circ, -2^\circ \leq \lambda_s \leq -10^\circ$$

By applying Equation (6.10), the optimized results are depicted in

Figure 6.11, indicating optimal angles of $\kappa_r = 75^\circ$, $\gamma_o = -6^\circ$ and $\lambda_s = -10^\circ$. The optimized surface roughness and tool wear are $Ra = 0.767\mu\text{m}$ and $VB = 22.2\mu\text{m}$.

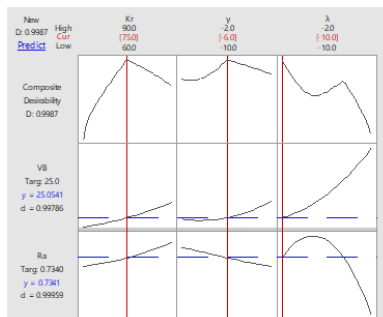


Figure 6.11 Simultaneous optimization of surface roughness and tool wear

c. Problem 3

A further research objective is the simultaneous minimization of surface roughness and tool wear. Therefore, Equation (6.9) is employed again,

where Y_i represents the output responses for surface roughness (Ra) and tool wear (VB), as described by Equations (6.1) and (6.2), respectively.

Subject to the constraints:

$$0.25 \mu\text{m} < Ra < 1.6 \mu\text{m}, 0 \mu\text{m} < VB < 0.3 \mu\text{m},$$

$$60^\circ \leq \kappa_r \leq 90^\circ, -2^\circ \leq \gamma_o \leq -10^\circ, -2^\circ \leq \lambda_s \leq -10^\circ$$

By applying Equation (6.9), the optimal results are shown in Figure 6.12, yielding the best tool angles at $\kappa_r = 60^\circ$, $\gamma_s = -10^\circ$ and $\lambda_o = -10^\circ$. The optimized surface roughness and tool wear are $Ra = 0.582 \mu\text{m}$ and $VB = 17.5 \mu\text{m}$, respectively.

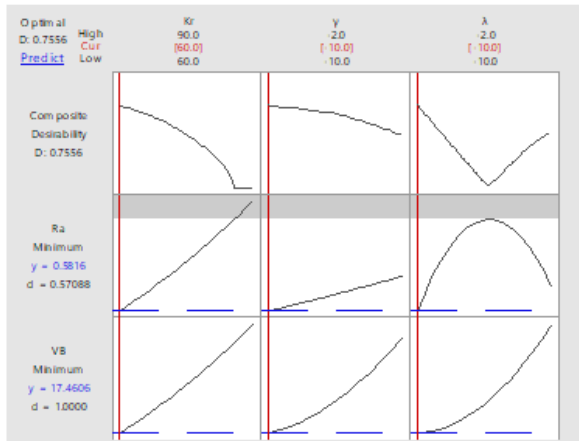


Figure 6.12 Simultaneous Optimization of Surface Roughness and Tool Wear

6.4.3 Comparison between standard tool angles and optimized tool angles

Table 6.10 indicates that experimental results for surface roughness and tool wear obtained with optimized tool angles showed reductions of 8.3% and 41.3%, respectively, compared to results achieved with standard tool angles.

Table 6.10 Comparison of experimental results for standard tool angles vs. optimized tool angles

Parameters		Standard Tool Angles	Optimized Tool Angles	Improvement
Input	K_r	91°	75°	
	γ_o	-6°	-6°	
	λ_s	-6°	-10°	
Output	Ra	0.836 μ m	0.767 μ m	↓ 8.3%
	VB	37.8 μ m	22.2 μ m	↓ 41.3%

6.5 Conclusion

This study has simultaneously analyzed the influence of tool angle parameters (side cutting edge angle, rake angle, and inclination angle) on surface roughness, tool wear, and cutting forces by integrating a mathematical model of hard-turning tool geometry with experimental data. The findings demonstrate that the role of these tool angles in hard turning significantly differs from their role in conventional turning. Specifically, the inclination angle is identified as the most critical factor in hard turning, whereas in conventional turning, the rake angle has the greatest influence.

Three optimization scenarios relevant to practical manufacturing applications have been successfully addressed within the hard-turning process.

CHAPTER 7:

CONCLUSIONS AND RECOMMENDATIONS

7.1 Conclusions

This study is the first to simultaneously evaluate the influence of tool geometry parameters, namely the side cutting edge angle (K_r), rake angle (γ_o), and particularly the inclination angle (λ_s) on three critical characteristics in hard turning: surface roughness, tool wear, and cutting forces. Based on experimental results and analytical observations, the main conclusions are as follows:

- In hard turning, due to the small feed rate and depth of cut, the cutting action occurs only at the tool nose radius. The inclination angle is the primary factor influencing the average local rake angle, accounting for 65.84%, followed by the rake angle at 31.43%, and the cutting edge angle at merely 0.98%. Consequently, for optimizing the hard turning process, focus should be directed toward adjusting the inclination angle and the rake angle. The cutting edge angle can be neglected due to its negligible effect. Increasing the negative rake and inclination angles increases the local rake angle of the cutting edge elements at the nose radius.
- There is a distinct difference in the roles of tool geometry parameters in hard turning versus conventional turning. In hard turning, the inclination angle has the greatest impact on surface roughness, tool wear, and cutting forces, whereas in conventional turning, the rake angle is typically the most significant parameter.
- The interactions of the cutting edge angle with the rake angle and with the inclination angle notably affect surface roughness. Surface roughness rises when the rake and inclination angles become more negative. However, once the inclination angle exceeds a certain threshold, surface roughness decreases. This is a novel and important finding in hard turning research. From these results, applying a larger negative inclination angle ($\lambda_s = -10^\circ$) is recommended to simultaneously reduce both surface roughness and tool wear.
- Tool wear decreases with increased negative rake and inclination angles.
- The radial force (F_y) is the largest force component, followed by the tangential force (F_z), while the axial force (F_x) is the smallest. Unlike conventional turning, where the tangential force is dominant, the radial force is dominant in hard turning.
- Experiment-based mathematical models for tool wear, surface roughness, and cutting force have been successfully developed.
- With the optimized tool angles ($K_r = 75^\circ$, $\gamma_o = -6^\circ$, và $\lambda_s = -10^\circ$), experimental results show reductions of 8.3% in surface roughness and

41.3% in tool wear, compared to the standard tool angles recommended by the manufacturer ($K_r = 91^\circ$, $\gamma_o = -6^\circ$ và $\lambda_s = -6^\circ$).

The proposed fixture design method provides an efficient solution for adjusting the tool geometry parameters of standard inserts, effectively enhancing the hard turning process.

A new geometric mathematical model of the hard turning process has been formulated, accurately representing the nature of the cutting action. Analytical findings from this model closely align with experimental results. This model can be integrated with other equations and mathematical models to calculate cutting forces, cutting temperature, and local tool wear for each cutting edge element and for the overall process. Furthermore, it can potentially be extended to analyze the turning of other difficult-to-machine materials.

7.2 Future research directions

Building upon the findings of this study, the following areas are suggested for future work:

- Hard turning of various hardened materials:
Further research could explore materials such as AISI 52100, AISI D2, AISI H13, and other difficult-to-machine steels to evaluate the general applicability of the optimized tool geometry.
- Hard turning with alternative cutting tools:
Additional investigations using Polycrystalline Cubic Boron Nitride (PCBN) inserts or other advanced cutting tool materials could be conducted to further improve machining performance.
- Comprehensive analysis of tool geometry and cutting conditions:
Examining the combined effects of both tool geometry parameters and cutting conditions on cutting forces, cutting temperature, tool wear and surface roughness to gain a more holistic understanding of the hard turning process.

LIST OF PUBLISHED WORKS

1. Le Hieu Giang, Mai Duc Dai and Pham Minh Duc. Investigation of Effects of Tool Geometry Parameters on Cutting Forces, Temperature and Tool Wear in Turning Using Finite Element Method and Taguchi's Technique. *International Journal of Mechanical Engineering and Applications*, 2016.
2. Pham Minh Duc, Le Hieu Giang, Mai Duc Dai and Do Tien Sy. An experimental study on the effect of tool geometry on tool wear and surface roughness in hard turning. *Advances in Mechanical Engineering (SCIE)*, 2020.
3. Pham Minh Duc, Mai Duc Dai and Le Hieu Giang. Modeling and Optimizing the Effects of Insert Angles on Hard Turning Performance. *Mathematical Problems in Engineering (SCIE)*, 2021.
4. Pham Minh Duc and Le Hieu Giang. Enhancing Hard Turning Performance: The Crucial Role of Cutting Parameters and Tool Geometry. *International Journal of Engineering Trends and Technology (Scopus)*, 2025.
5. Pham Minh Duc, Le Hieu Giang and Van Thuc Nguyen. Analyzing Cutting Temperature in Hard Turning Technique with Standard Inserts through Both Simulation and Experimental Investigations. *Applied sciences (SCIE)*, 2025.
6. Van Thuc Nguyen, Nguyen Quang Hien, Pham Minh Duc, Tran Duy Nam, Van Huong Hoang and Van Thanh Tien Nguyen. Atomistic Insight into the Effects of Collision Angle on the Characteristics of Cu-Ta Joining by Explosive Welding. *Metals (SCIE)*, 2025.